Chapter 1
The Influence of Entrained Air on the Dynamic Compressive Performance of Conventional Concrete

Mahmoud M. Awd Allah*, **Mohamed A. Abbas**, **Brett A. Williams**, **William F. Heard**, **and Xu Nie**

Abstract Freeze-thaw damage is a common form of deterioration in concrete that happens when it is subjected to frequent cycles of freezing and thawing, mainly in cold weather. This kind of damage mostly affects the durability of concrete, causing scaling, cracking, and spalling that over time can compromise the structural integrity. One of the useful approaches to decreasing freeze-thaw damage is by adjusting permeability, such as introducing entrained air in the concrete mix acting as pressure-relief zones when water inside the concrete freezes and expands. This method does not directly reduce permeability but mitigates the influence of any water entrapped in the concrete. Understanding the relationship between the entrained air percent and dynamic behaviors of concrete facilitates more effective use of materials. By studying this connection, designers can determine the acceptable percentage of air that doesn't significantly compromise the concrete's performance. It is therefore the goal of this study to answer the question: To what extent can air content affect the dynamic compressive performance of conventional concrete? Subsequently, cylindrical specimens with different air content percentages were developed and tested under dynamic strain rates. For the dynamic testing, a 2-inch diameter Kolsky compression bar system with well-designed pulse shapers was used to enable the constant strain rate deformation and dynamic stress equilibrium conditions. The results revealed that the air content imposes significant impacts on the dynamic compressive performance of conventional concrete.

Keywords Heterogeneous material · Freeze-thaw damage · Permeability · High strain rate · Split Hopkinson pressure bar

Introduction

Concrete is the most widely used building material due to its cost-effectiveness, durability, mechanical properties, and design flexibility [1]. However, it faces challenges that affect its performance and sustainability, particularly freeze-thaw (FT) damage in regions with fluctuating temperatures around freezing point [2]. During freezing, internal moisture in concrete expands, creating internal pressures that can cause micro cracks and damage. In the thaw cycle, the ice melts, and the concrete contracts, further stressing the structure [3]. Repeated FT cycles worsen the damage, weakening key properties like mass, elasticity, strength, and fracture toughness.

Permeability is a key factor in FT damage, especially in materials like concrete and soil. It refers to a material's ability to allow fluids, such as water, to pass through [4]. High permeability allows fluids to pass through easily, while low permeability means fluids flow slowly or are blocked. This property is critical in fields like geology, civil engineering, and environmental science, as it influences water movement, drainage, and structural stability. To address FT damage in concrete related to permeability, a variety of solutions have been developed and implemented to improve its resistance and durability. One of the solutions is design the concrete mix by incorporating air-entraining agents into the mix [5]. These agents create microscopic air bubbles that allow for the expansion of freezing water without causing damage. For this instant, according to Peng et al. [6] the inclusion of entrained air significantly enhances frost resistance, allowing materials to withstand up to 300 FT cycles. This improvement is attributed to the air bubbles created during the mixing process, which act as a cushion, absorbing the stress generated by the expansion of freezing water within the material's pores.

Mahmoud M. Awd Allah · Mohamed A. Abbas · Xu Nie
Mechanical Engineering Department, Southern Methodist University, 6425 Boaz Lane, Dallas, TX 75205, USA
e-mail: mawdallah@smu.edu; maabbas@mail.smu.edu; xnie@mail.smu.edu

Brett A. Williams · William F. Heard
Army Engineer Research and Development Center, 3909 Halls Ferry Rd, Vicksburg, MS 39180, USA
e-mail: brett.a.williams@erdc.dren.mil; william.f.heard@erdc.dren.mil

Paul Allison et al. (eds.), *Dynamic Behavior of Materials, Vol. 1*, Conference Proceedings of the Society for Experimental Mechanics Series, https://doi.org/10.13052/97887-438-0827-5_1

Additionally, Tanesi and Meininger [7] investigated the FT resistance of concrete with minimal air content by utilizing Vinsol resin and synthetic air-entraining agents. The findings revealed that concrete with an air content of up to 3.5% exhibited satisfactory FT performance when combined with Vinsol resin-based air-entraining agents. This suggests that the specific properties of Vinsol resin contribute positively to the air-entraining process, enhancing the material's resistance to FT cycles. Later on, Hang et al. [8] pointed out that concrete displays the best FT resistance at air content of 4.6 : 6.5%. Moreover, the addition of entrained air affects the concrete's fluidity and compressive strength. The concrete's fluidity first rises and then falls with an increase in entrained air dosage, and the compressive strength decrease. It is also noteworthy that when comparing concrete created using recycled aggregate to concrete made with virgin aggregate, the use of air entrainment and polypropylene fibers has proven to be similarly successful in providing FT endurance, as stated by Richardson et al. [9].

Considering the literature listed above, there is a lack of experimental studies on the dynamic compressive performance of conventional concrete with entrained air. To address this, cylindrical specimens with air content percentages of 2 and 7% were developed and tested under dynamic strain rates. A 2-inch diameter Kolsky compression bar system, equipped with pulse shapers, was used for the dynamic testing to maintain constant strain rate deformation and dynamic stress equilibrium conditions.

Methodology

Materials

The material being utilized in this study is conventional concrete, that has been developed by the U.S. Army Engineer Research and Development Center (ERDC). Conventional concrete, known for its strength, versatility, and durability, is formulated by combining specific proportions of various ingredients such as cement, aggregates, water, and admixtures. Table 1 provides a detailed breakdown of the mixture proportions for the individual components of this particular concrete.

Specimens preparation

A four-step process described by Heard et al. [10] was used to prepare all specimens used in this work. Once the material is fully cured, the process begins by core drilling long cylinders with 44.60-mm in diameter from the bulk material. These cylinders are then sectioned into individual pieces using a Beuhler Delta-EB 260 manual abrasive cutter. Subsequently, the ends of the specimens undergo grinding using a Harig 618 auto-step precision surface-grinder to enhance the flatness and parallelism of the ends. Finally, each specimen undergoes polishing in a high-precision P.R. Hoffman PR-1 double-sided lapping machine to achieve their final length of 22.40 mm. This particular process ensures maximum flatness and parallelism of the specimen ends, thereby minimizing stress concentrations at the specimen/bar interfaces.

Table 1 The mixture proportions for the concrete used in this work.

Component	Unit	Amount (per one cubic yard)
Type 1L Cement	lbs	517.5
#89 Limestone	lbs	1558.7 (absorption: 0.30%)
Concrete Sand	lbs	1496.3 (absorption: 0.50%)
Water	lbs	290.9
Admixture 1 – Viscocrete 2100	lbs	2.19
Admixture 2 – Sikatard	lbs	2.91
Admixture 3 – Sika Air	lbs	0.20
Water to cement ratio (w/c)	-	0.57

Test description

The dynamic uniaxial compression tests were conducted using a 2-inches diameter Kolsky compression bar apparatus. The Kolsky Compression Bar, also referred to as the Split-Hopkinson pressure bar, is a dependable method for evaluating material response under high strain-rate uniaxial compression. The method is based on one dimensional stress wave theory in elastic solids. In this test setup, the specimen is placed between two elongated elastic rods, forming the conventional Kolsky compression bar assembly, aligned along a shared axis. A gas gun typically propels a striker, accelerating it to collide with the incident bar, which is one end of the first rod. The impact generates a compressive stress wave that travels along the incident bar towards the specimen. Upon reaching the specimen end, a portion of this stress wave reflects back up the incident bar, while the rest transmits into the specimen. This transmission occurs due to a shift in mechanical impedance at the specimen interface. The specimen is deformed when the transmitted stress wave passes through it and enters the second rod, also referred to as the transmission bar. Resistive strain gauges attached to the bar surfaces allow for the measurement and recording of the stress waves as they move along the bars. A Wheatstone bridge circuit is coupled to the strain gauges, and a high-resolution digital oscilloscope records the output voltage. The oscilloscope's recorded waves can be used to compute the specimen's stress and deformation history if the stress waves are assumed to be one-dimensional and non-dispersive. A well-designed experiment can satisfy these two essential assumptions. It has been demonstrated that the one-dimensional wave propagation assumption holds true provided that the incident and transmission bars are long enough to enable the radial stress distribution to become uniform. Wave dispersion effects can become significant when the incident loading wave comprises components of different frequencies. However, studies have indicated that employing proper pulse shaping techniques to eliminate higher frequency components of the incident loading wave can render the effects of wave dispersion negligible [11]. Figure 1 represents a schematic diagram of the Kolsky compression bar used in the present work.

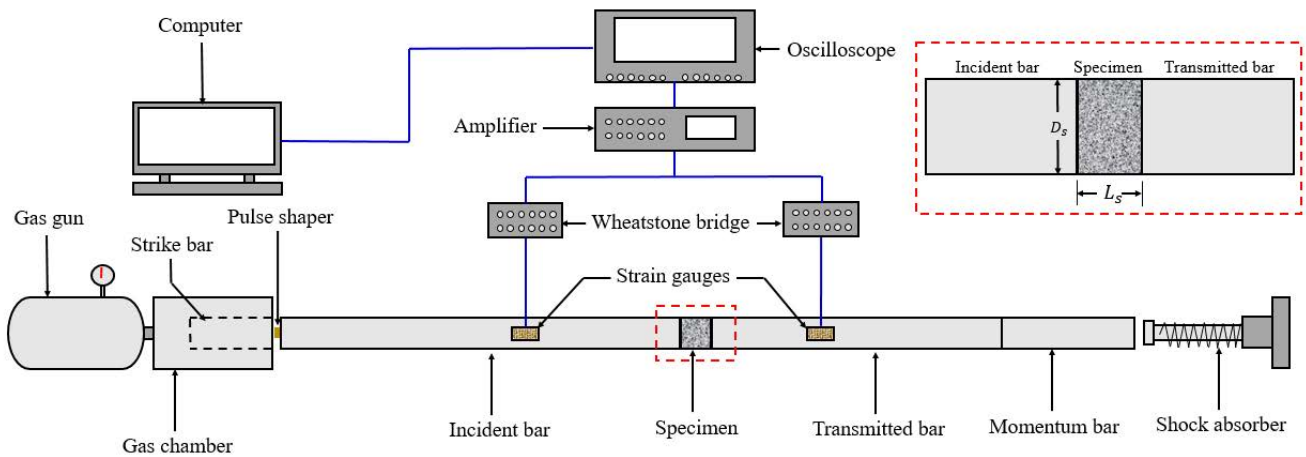

Fig. 1 Schematic diagram of Kolsky bar.

Results and Discussions

To evaluate the average dynamic compressive strength of the studied material with different air percentages, five samples were tested using a Kolsky bar apparatus under monotonic compressive loading conditions. The dynamic compressive strength for each specimen was determined by identifying the maximum stress recorded during the loading phase. This maximum stress represents the material's peak resistance to dynamic compression prior to fragmentation. Figure 2 illustrates the original waveforms obtained from the oscilloscope during the monotonic loading tests, including the incident, reflected, and transmitted wave components. Additionally, Figure 2 presents the calculated bar stress histories at two critical locations: the incident bar end ($\sigma_I + \sigma_R$), where the sum of incident and reflected stresses is analyzed, and the transmission bar end (σ_T), where the transmitted stress is recorded.

The strain rate of the specimen is directly proportional to the behavior of the reflected wave during the loading process. This relationship allows the strain rate history during monotonic loading to be categorized into three distinct stages, each representing a specific phase of deformation and failure. The first stage is characterized by a progressive increase in the amplitude of the reflected wave. This increase corresponds to a period of non-constant strain rate deformation, which arises due to the axial acceleration of the specimen particles. During this phase, the material is transitioning from a state of rest to dynamic loading, and the strain rate varies as the specimen begins to resist the applied load. In the second stage, the reflected wave profile reaches a plateau, indicating the establishment of a constant strain rate. The plateau demonstrates a stable deformation response, where the applied stress and resulting strain rate remain balanced [12]. This stage is critical for accurately capturing the dynamic behavior of the material under controlled loading conditions. The third stage is marked by a sharp and dramatic increase in the amplitude of the reflected wave. At this point, the wave no longer represents the strain rate of the specimen. Instead, it reflects the free motion of the bar's end face, which occurs as the specimen fails and

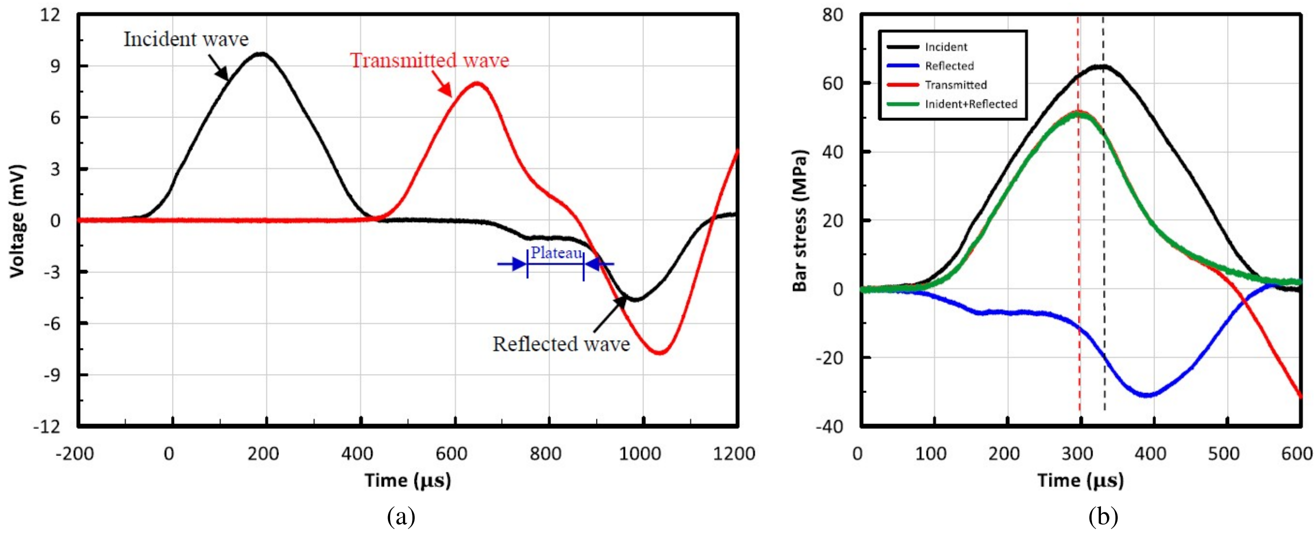

Fig. 2 (a) the original signals recorded by strain gauges and (b) the shifted waves.

can no longer sustain the applied load. This phase signals the peak of the loading process and the complete fragmentation of the specimen. Additionally, the transmitted wave provides further insight into the material's response. The transmitted wave reaches its peak amplitude earlier than the incident wave, a phenomenon attributed to the material's inherent softening behavior. The trailing portion of the transmitted wave, results from this softening effect and highlights the gradual reduction in the material's ability to carry load as failure progresses.

Figures 3 and 4 represent the engineering stress-strain curves and the corresponding strain rate histories for the tested specimens with 2 and 7% under monotonic compression loading, respectively. It is clear that both the percentages demonstrate an initial elastic response, which transitions into plastic strain hardening as the material deforms toward its peak stress. The transition from elastic to plastic behavior is primarily attributed to the propagation and combination of micro cracks. This mechanism mitigates the high lateral tensile stress concentrations that develop at the crack tips under compressive loading conditions. These micro cracks play a vital role in accommodating the compressive forces and contribute to the overall deformation characteristics of the material. The heterogeneous composition of the concrete material introduces some variability in the dynamic mechanical response observed across individual specimens. This variability arises from the inherent differences in the material's microstructure, such as aggregate distribution and pore size, which influence its strength and deformation behavior under dynamic loading. Despite the inherent variability, the experimental data shown in Figures 3 and 4 demonstrate a notable reduction in scatter within the stress-strain responses. This enhanced consistency can largely be attributed to the implementation of pulse shaping techniques. These techniques are essential in ensuring that the loading conditions remain both controlled and repeatable [13]. By effectively smoothing the incident wave, pulse shaping minimizes fluctuations and irregularities in the applied load, promoting a more uniform distribution of stress across the specimen. As a result, these techniques help to reduce experimental artifacts, leading to more reliable, consistent, and reproducible outcomes that strengthen the overall validity of the experimental findings.

Additionally, Table 2 demonstrates the average mechanical properties of concrete specimens with varying air content percentages. The data clearly indicates that the dynamic compressive performance of the specimens with 2% air content is significantly higher, showing a 19.63% increase compared to those with 7% air content. This difference in performance suggests that the air content plays a significant role in the mechanical behavior of concrete under dynamic loading conditions. The improved performance of the specimens with lower air content is the reduction in porosity and air voids within the concrete matrix. Concrete with higher air content typically has an increased number of microscopic voids, which can act as points of weakness under compressive stress. These voids can reduce the overall density and structural integrity of the material, making it more prone to deformation and failure when subjected to dynamic loads, such as impact or high strain rate compression. In contrast, reducing the air content in the concrete leads to a denser material with fewer voids, which enhances its ability to distribute applied stresses more uniformly throughout the matrix. This results in a stronger, more resilient material that is better equipped to withstand dynamic forces. Additionally, lower air content often leads to improved bonding between the cement paste and aggregates, further strengthening the concrete's overall mechanical properties. Furthermore, the improved performance of the 2% air content specimens could be the reduction in the potential for FT damage. Concrete with excessive air content may exhibit greater susceptibility to FT cycles, especially in cold climates. Although air entrain-

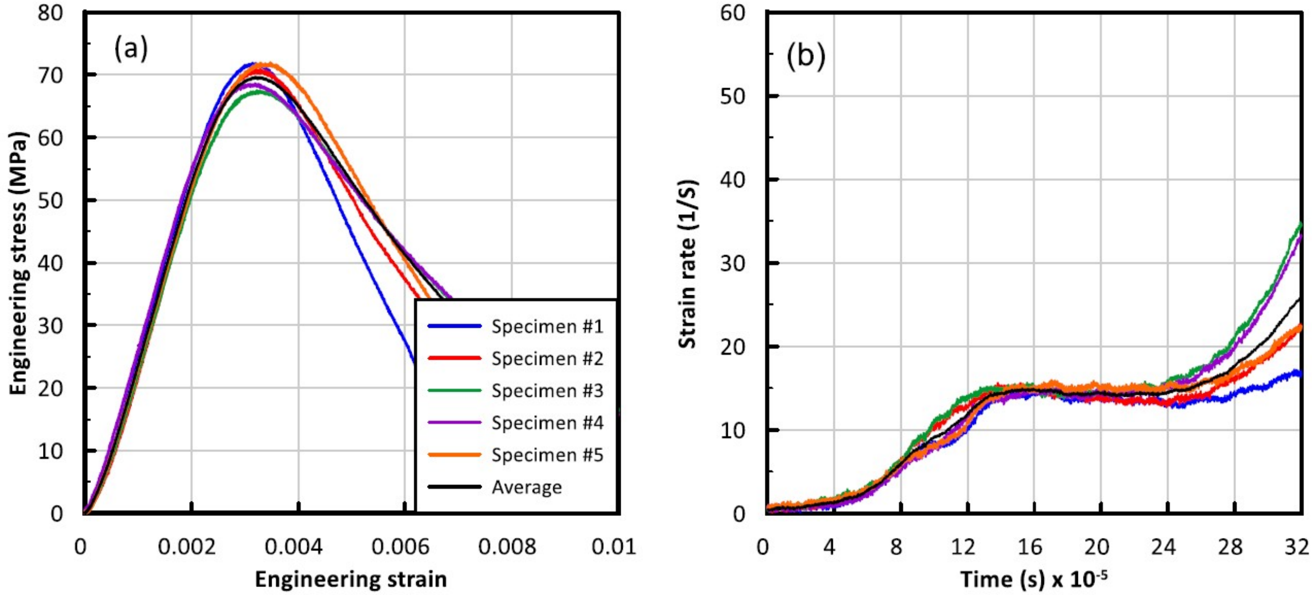

Fig. 3 Dynamic performance (a) compressive stress-strain and (b) strain rate history for specimens with 2% air percent.

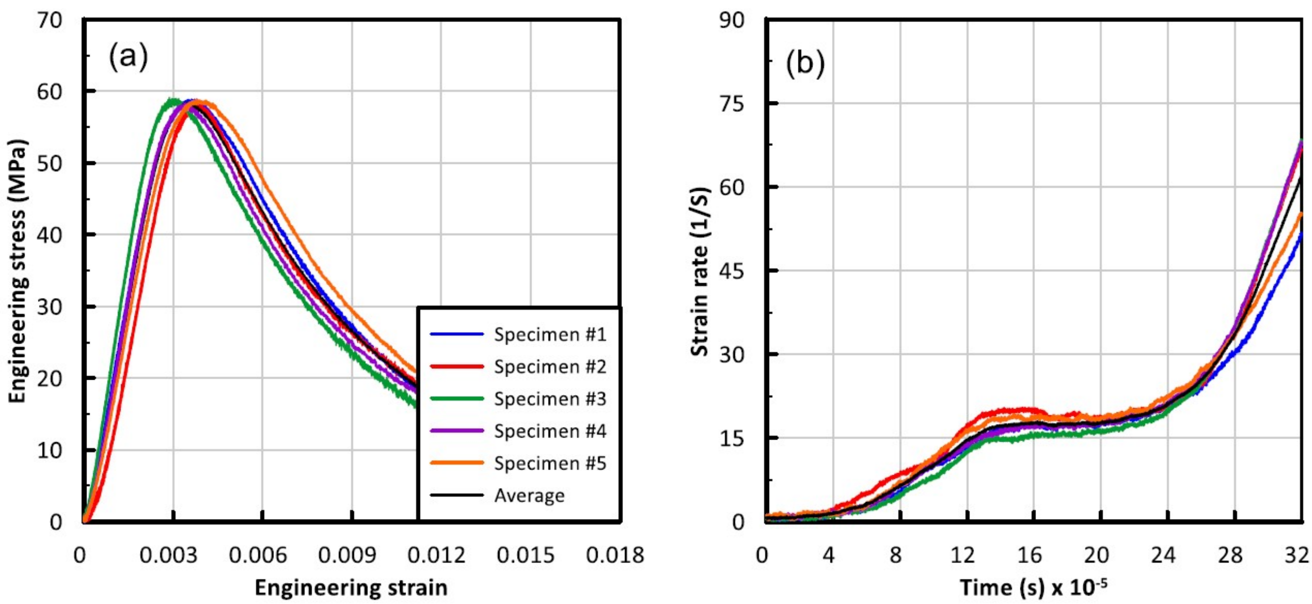

Fig. 4 Dynamic performance (a) compressive stress-strain and (b) strain rate history for specimens with 7% air percent.

ment is typically used to improve the FT resistance of concrete, an optimal balance must be maintained. Too much air can lead to excessive void spaces that, while initially providing some resistance to freezing and thawing, could also reduce the concrete's overall strength and performance in dynamic conditions. These findings emphasize the importance of controlling air content in concrete mixtures to optimize their mechanical properties, particularly for applications that require resistance to dynamic loads and compressive forces. This result is consistent with the findings of Ge et al. [14], who reported that properly managing air content ensures that the concrete achieves a balance between durability, strength, and performance, leading to more reliable results in practical engineering applications.

Moreover, Table 2 displays the plastic strain at the peak stress for the concrete specimens with 2% air content is 0.0033, while for those with 7% air content, it is 0.0035. Although the strain values at peak stress are similar, with only a slight difference of 0.0002, it is important to recognize that the overall mechanical behavior of the specimens is still influenced by the air content. Therefore, even though both materials may undergo similar amounts of plastic deformation at peak stress, the concrete with lower air content is still better suited for dynamic applications due to its overall superior compressive strength.

Table 2 The average mechanical properties of the tested specimens.

Air percent	Data	Strain rate (1/S)	Dynamic compressive strength (MPa)	Plastic strain at the peak stress	Density (kg/m^3)
2%	Avg.	14.24	70.58	0.0033	2368.20
	SD	0.74	2.07	0.0001	27.88
	CV, %	5.17	2.94	3.4975	1.18
7%	Avg.	17.86	59.00	0.0035	2288.00
	SD	1.11	0.38	0.0004	8.54
	CV, %	6.24	0.65	10.89	0.37

Conclusions

This study explores the impact of varying air content percentages on the compressive dynamic performance of conventional concrete. For this reason, cylindrical specimens with air content levels of 2 and 7% were prepared and subjected to dynamic strain rate testing. Based on the analyses, the following findings were drawn: The importance of carefully considering and optimizing air content percentages to enhance the dynamic performance of concrete. Also, reducing air content in concrete significantly enhances the dynamic compressive strength. However, air content variations showed no notable impact on the plastic strain at peak stress.

Conflict of interest statement No possible conflicts of interest were disclosed by the authors.

Data availability statement The corresponding author will send the datasets generated and/or analyzed in the current work upon reasonable request.

References

1. Thomas, C., J. Setién, J. Polanco, P. Alaejos, and M.S. De Juan, Durability of recycled aggregate concrete. Construction and building materials, 2013. 40: p. 1054-1065.
2. Shah, H.A., Q. Yuan, and S. Zuo, Air entrainment in fresh concrete and its effects on hardened concrete-a review. Construction and Building Materials, 2021. 274: p. 121835.
3. Bogas, J.A., J. De Brito, and D. Ramos, Freeze–thaw resistance of concrete produced with fine recycled concrete aggregates. Journal of Cleaner Production, 2016. 115: p. 294-306.
4. Amriou, A. and M. Bencheikh, New experimental method for evaluating the water permeability of concrete by a lateral flow procedure on a hollow cylindrical test piece. Construction and building materials, 2017. 151: p. 642-649.
5. Shi, Y., H. Yang, S. Zhou, A. Wang, and X. Lv, Effect of atmospheric pressure on performance of AEA and air entraining concrete. Advances in Materials Science and Engineering, 2018. 2018(1): p. 6528412.
6. Peng, G.-F., Q. Ma, H.-M. Hu, R. Gao, Q.-F. Yao, and Y.-F. Liu, The effects of air entrainment and pozzolans on frost resistance of 50–60 MPa grade concrete. Construction and Building Materials, 2007. 21(5): p. 1034-1039.
7. Tanesi, J. and R. Meininger, Freeze-thaw resistance of concrete with marginal air content. Transportation research record, 2007. 2020(1): p. 61-66.
8. Hang, M., L. Cui, J. Wu, and Z. Sun, Freezing-thawing damage characteristics and calculation models of aerated concrete. Journal of Building Engineering, 2020. 28: p. 101072.
9. Richardson, A., K. Coventry, and J. Bacon, Freeze/thaw durability of concrete with recycled demolition aggregate compared to virgin aggregate concrete. Journal of Cleaner Production, 2011. 19(2-3): p. 272-277.
10. Heard, W., B. Martin, X. Nie, T. Slawson, and P. Basu, Annular pulse shaping technique for large-diameter Kolsky bar experiments on concrete. Experimental Mechanics, 2014. 54: p. 1343-1354.
11. Shemirani, A.B., R. Naghdabadi, and M. Ashrafi, Experimental and numerical study on choosing proper pulse shapers for testing concrete specimens by split Hopkinson pressure bar apparatus. Construction and Building Materials, 2016. 125: p. 326-336.
12. Abbas, M.A., B.A. Williams, W.F. Heard, and X. Nie, Residual mechanical properties of high strength concrete BBR9 subjected to dynamic uniaxial compressive loading. Cement and Concrete Research, 2024. 180: p. 107488.
13. Chen, X., L. Ge, J. Zhou, and S. Wu, Experimental study on split Hopkinson pressure bar pulse-shaping techniques for concrete. Journal of Materials in Civil Engineering, 2016. 28(5): p. 04015196.
14. Ge, X., Y. Ge, Q. Li, X. Cai, W. Yang, and Y. Du, Effect of low air pressure on the durability of concrete. Construction and Building Materials, 2018. 187: p. 830-838.